JOURNAL OF MATERIALS SCIENCE 1 (1966) 238-248

Crystal Structure Transformations of Alkali Sulphates, Nitrates and Related Substances*: Thermal Hysteresis in Reversible Transformations

K. J. RAO, C. N. R. RAO
Department of Chemistry, Indian Institute of Technology, Kanpur, India

Received 29 March 1966

Reversible phase transformations of alkali sulphates, alkali nitrates, and various other inorganic substances have been studied by making use of differential thermal analysis. Thermodynamic and kinetic data on the transformations have been obtained. Thermal hysteresis in reversible transformations has been examined, and the magnitude of hysteresis is shown to be related to the volume changes accompanying the transformations. The origin of hysteresis probably lies in the strain energies associated with the transformations. Approximate strain energies have been estimated from the analysis of the DTA data. On the basis of considerations from the theory of elasticity, it is possible to show that the strain energy is a function of ΔV. Thermodynamic considerations show that the strain energy is related to $\Delta T \times \Delta S$.

1. Introduction

All the alkali sulphates undergo polymorphic transformations [1], and there are several papers in the literature describing the crystallography and some of the thermodynamic aspects of these transformations. The information regarding the reversibility, quantitative thermodynamic, and kinetic aspects of the transformations is, however, limited. We have now investigated all these three aspects of polymorphic transformations of alkali sulphates, employing precision differential thermal analysis

Alkali metal nitrates with the exception of lithium nitrate exhibit polymorphic transformations [1, 2]. Crystallographic aspects of these transformations have been studied in detail, particularly in view of the ferroelectricity associated with some of the transformations. Although some thermodynamic data on these transformations are available, it was considered worthwhile to examine the reversibility of these transformations as well as the kinetic aspects.

While the transformations of alkali sulphates and nitrates have been classified as "reversible" transformations, considerable hysteresis effects are seen in these transformations either in terms of intermediate phases in one of the directions (as in sodium sulphate and potassium nitrate) or in terms of the fairly large differences in transformation temperatures of the forward and reverse paths. It was one of our main interests to study the thermal hysteresis in reversible transformations, and suggest a suitable model to account for such effects in reversible transformations. For this purpose, we have examined the crystal structure transformations of a number of inorganic solids, apart from those of alkali sulphates and nitrates. Another point of interest in the present study was to examine the applications and limitations of precision differential thermal analysis as a tool in the quantitative evaluation of the thermodynamic and kinetic data of crystal structure transformations.

All the transformations examined in the present study are likely to be nucleation-and-growth transformations, and most of them are quite sluggish. The hysteresis phenomenon

---

*Taken in part from Ph.D. thesis of K. J. Rao, to be submitted to the Indian Institute of Technology, Kanpur.

discussed here may be of relevance to the study of both the nucleation-and-growth and martensite transformations in metal systems.

2. Experimental

Most of the chemicals employed in this study were of analytical grade and were commercially available. Caesium sulphate, rubidium sulphate, caesium nitrate, and rubidium nitrate were prepared starting from the corresponding carbonates. Ytterbium borate was prepared by heating a stoichiometric mixture of boric acid and ytterbium oxide to 900° C. All the substances, in powder form, were dried and stored in desiccators before subjecting them to *differential thermal analysis* (DTA).

DTA was carried out employing a recording Aminco Thermoanalyser, fitted with a temperature programmer, a differential amplifier, and an automatic voltage stabiliser. A thermocouple in series with the block thermocouple was immersed in an ice-water mixture so as to maintain 0° C as the reference temperature. Constant heating rates were obtained by employing appropriate gear clusters and initial applied voltages on the furnace. The DTA curves were recorded under conditions where the heating and cooling rates were nearly identical. All the substances studied were polycrystalline, and alumina was used as the reference. Typical DTA curves obtained in the present study are shown in fig. 1.

The enthalpy of transformation, ΔH^0, was obtained from the peak areas in the DTA curves [3-6], employing copper sulphate pentahydrate [6] and quartz [9] as references. In the case of the transformation of alkali sulphates, potassium sulphate [10] was also used as an internal standard. It was established that, by this technique, reliable values for heats of phase transformations could be obtained. For example, the heats of transformation of potassium nitrate (II → I) and rubidium nitrate (IV → III) were obtained as 1.2 and 0.95 kcal/mole respectively, compared to the calorimetric values of 1.2 [7] and 0.92 [8] kcal/mole. In the case of the $\mathrm{P}m3m \rightarrow \mathrm{F}m3m$ transformation of caesium chloride [11], the ΔH^0 was found to be 580 ± 100 cal/mole, which agrees well with the calorimetric value. The enthalpy values obtained in this study have an uncertainty of $\pm 15\%$. The enthalpy values in the case of second order transformations which occur over a very wide temperature range were not reliable, as will be discussed later. From the DTA curves, the peak temperatures, T_p (at which the transformation goes to completion), were obtained, and wherever possible the temperature of initiation of transformation, T_i, was also noted. The data on T_p and T_i were recorded both for the forward (T_p^f and T_i^f) and the reverse (T_p^r and T_i^r) directions.

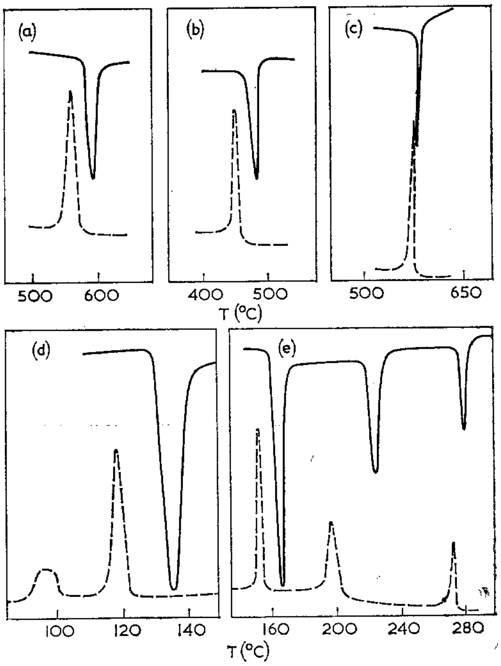

Figure 1 Typical differential thermograms of reversible phase transformations: (a) Li_2SO_4; (b) CsCl; (c) quartz; (d) KNO_3; (e) $RbNO_3$. Broken curves correspond to reverse transformations (cooling curves), while the full curves correspond to forward transformations (heating curves).

The energies of activation, E_a, could be obtained by the method of Borchardt and Daniels [12] within an uncertainty of $\pm 15\%$. Although there is considerable controversy regarding the evaluation of k, first order rate constant, and E_a from DTA curves, it may be reasonable to compare values of E_a in a related series of systems [11]. Further, obtaining good linear plots of log k versus $1/T$ seems to serve as a fairly satisfactory criterion for obtaining meaningful values of E_a. Such linear plots were found in the present study when the DTA peaks were subjected to the analysis of the type suggested by Borchardt and Daniels [12]. The fraction transformed at any one temperature (fig. 2) was evaluated by taking the ratio of the height of the curve at the temperature (from the base line) and the peak height.

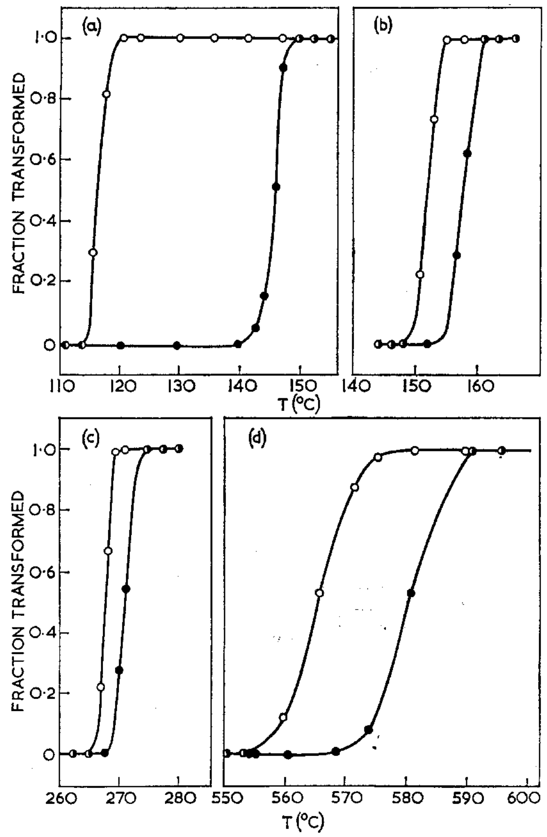

Figure 2 Typical hysteresis loops obtained in reversible transformations: (a) NH_4Cl ($Pm3m \rightarrow Fm3m$); (b) $CsNO_3$ (II → I); (c) $RbNO_3$ (II → I); (d) LiS_2O_4 (II → I).

3. Results and Discussion

3.1. Crystal Structure Transformations of Alkali Sulphates

Relevant crystallographic data, temperatures, enthalpies, and energies of activation for the phase transformations of alkali sulphates are given in table I. With the exception of lithium sulphate [13], where the transformation is from a monoclinic to a cubic structure, all the alkali sulphates show the transformation from the low temperature orthorhombic structure to the high temperature hexagonal structure. In the case of sodium sulphate, however, in the transformation of the low temperature orthorhombic form to the high temperature hexagonal form, at least two or three intermediate metastable forms have been reported, and these intermediate forms are not seen in the reverse direction [17, 18, 24-27]. On cooling, the high temperature hexagonal form of sodium sulphate reverts to an intermediate orthorhombic form rather than the initial low temperature orthorhombic form [18, 26].

Both the temperature and the heat of transformation show a marked decrease going from lithium sulphate to sodium sulphate. The temperature of transformation then progressively increases from sodium to caesium sulphate, while the heat of transformation decreases. The progressive variations of the heats and temperatures of transformation are understandable, since the crystallographic changes are similar and all the crystal structures are isomorphous.

The heat of transformation decreases in the same order as the increase in the volume available per sulphate ion in the lattice or the radius ratio (table I), and in the extreme case of caesium sulphate, where the volume per sulphate ion is very large, the ΔH^0 is also very small. The energy of activation of the transformation also decreases in the same direction as the ΔH^0. In the transformation of sodium sulphate, the values of energies of activation could not be evaluated, because of the occurrence of a number of intermediate phases, and values for only two transformations are shown in table I.

The differential thermograms (heating curves) of sodium sulphate showed two unique peaks centred around 225 and 265° C, and three marked shoulders between these two temperatures. By decomposition of the area under the thermogram into five additive areas, the heats for the individual transformations were estimated (table I). The total heat of transformation (2200 cal) agrees fairly well with the calorimetric value (2430 cal) of Coughlin [23a]. The heat of transformation found for other sulphates agree well with the early estimates of Fischmeister [23b].

The variation in transformation temperatures in alkali sulphates has been interpreted in terms of anion-cation polarisation effects (contrapolarisation [30]), and also in terms of the strengths of the metal-oxygen bonds [28, 29]. Variation in bond distance during the transformation seems quite possible, and such a variation has been noticed in the case of sodium nitrite [31]. Further, it is also possible that the rotation of the sulphate ion, which should give rise to second-order effects, is also associated with the observed transformations [32a]. The decrease in the temperature, the ΔH^0 and the E_a of transformation with the increase in the

TABLE I Reversible phase transformations of alkali sulphates.

M_2SO_4 M	Transformation	T_p^f (°C)	T_p^r (°C)	ΔH° (cal/mole)	E_a (kcal/mole)	ΔV (cm^3/mole)	$V^{(a)}$ (Å^3)	$\rho^{(c)}$
Li	Monoclinic (II) →	590	555	6900	250	3.81	80.2	
	cubic (I) [13]						86.54	0.30
Na	Orthorhombic (V, IV, III, II) →						82.6	0.44
	hexagonal (I) [14-17]						86.47	
	IV → III	225	—	320	100$^{(b)}$			
	V → III	238	—	280	—	2.34		
	IV → II	246	—	380	—			
	IV → I	255	—	600	—			
	III → I	265	231	620	90			
K	Orthorhombic (β) →	579	571	2142$^{(d)}$	230	1.55	88.65	0.62
	hexagonal (α) [10, 17-19]						92.9	
Rb	Orthorhombic (β) →	640	633	350	220	10.68	94.0	0.69
	hexagonal (α) [20-23b]						112.28	
Cs	Orthorhombic (β) →	698	690	150	190	9.64	100.9	0.78
	hexagonal (α) [20-23b]						119.06	

(a) Volume available for $SO_4^{=}$ ion calculated from the unit cell dimensions and ionic radii.
(b) E_a could not be evaluated for all the transformations.
(c) ρ is the radius ratio.
(d) ΔH° of transformation of K_2SO_4 was used as an internal standard. The value indicated is from Kelly, as quoted in reference 10.

volume available for the sulphate ion is indicative of the reconstructive nature of the transformation [32b] and possible role of rotation of the sulphate ion in determining the characteristics of the transformation. It appears likely that in the case of rubidium and caesium sulphates, where the ΔH^0 is small and the volume available for the sulphate ion is large, the transformations have considerable second order contributions. The transformation temperatures are sufficiently high in these cases for rotation to occur. It is possible that the measured ΔH^0 values are small in these cases due to the occurrence of the transformations over a wide temperature range. This difficulty in the measurement of ΔH^0 by DTA has been pointed out even in the transformation of potassium sulphate [12].

Some preliminary experiments on mixed sulphates of lithium and sodium as well as of potassium and rubidium also support these observations. Incorporation of 5% sodium in lithium sulphate or rubidium in potassium sulphate decreases the temperature as well as the ΔH^0 of transformation, as can be seen from the data below.

Compound	T_p^f (°C)	T_p^r (°C)	ΔH^0 (kcal/mole)
Li_2SO_4	590	555	6.9
Li_2SO_4 + 2 wt % Na_2SO_4	579	540	5.0
Li_2SO_4 + 5 wt % Na_2SO_4	570	530	3.5
K_2SO_4	579	572	2.1
K_2SO_4 + 5 wt % Rb_2SO_4	575	573	2.0

[Continued in next column

The cation impurities seem to be entering the lattice substitutionally as expected, and the higher radius ratio of the impurity has marked effect on the transformation characteristics.

3.2. Crystal Structure Transformation of Alkali Nitrates

Important crystallographic data, transformation temperatures as well as the heats and energies of activation of the transformations of alkali nitrates are summarised in table II. With the exception of sodium nitrate [33-35], the transformations of alkali nitrates are associated with ferroelectricity [41-45]. In potassium nitrate, ferroelectricity is found in the metastable intermediate phase, while cooling the high-temperature form [36-38] (~125° C). All the measured heats of transformation are small in these nitrates, typical of second order transformations. It has been pointed out in the case of sodium nitrate that the transformation is probably associated with nitrate ion rotation [32a, 33]. In potassium nitrate, recent spectroscopic studies [46] have indicated that anion rotation may be associated with the transformation.

The ΔH^0 value found from the DTA in the case of sodium nitrate is very much lower than that determined by calorimetry [47]. This is an inherent difficulty associated with the dynamic nature of the measurement employed in DTA. Since second order transformations are likely to take place over a wide range of temperature, the observed area under the DTA peak will be small and will not correspond to the true heat of transformation. The same disagreement is encountered between the calorimetric and DTA values of ΔH^0 for the transformations of rubidium nitrate [8] (III → II) and caesium nitrate [45], where ferroelectricity has been observed. It is, however, gratifying that where the anion rotation may not be playing an important role, as in the potassium nitrate (II → I) transformation or in the rubidium nitrate (IV → III) transformation, the DTA values agree fairly well with the calorimetric data. It appears that the DTA values of ΔH^0 can be relied upon only where there is little contribution from second order effects.

The temperatures, heats and energies of activation do not vary systematically in the case of alkali nitrates (table II), and it is difficult to explain these changes simply in terms of the contrapolarisation [30] effects or metal-oxygen bonding [28-29].

3.3. The Energy of Activation of the Transformations

The energies of activation throw some light on the structural mechanism of the transformations. Thus, reconstructive transformations which involve the breaking of the primary coordination [32b] directly or indirectly are associated with large values of E_a. The P*m*3*m*-F*m*3*m* transformation of caesium chloride [11] shows a high value of E_a (160 kcal/mole), even though a dilatational mechanism is supposed to be operative. The lattice energy differences of the two phases (ΔH^0) are generally small in these transformations, and the high values of E_a indicate that the mechanism involves reconstruction. Most of the E_a is likely to be spent in the nucleation step. The transformations for which E_a has been determined in the present study (tables I and II) probably are of reconstructive type, since they show high E_a values.

3.4. Volume Change in the Transformations

Since all the transformations studied are accompanied by marked changes in molar volume, ΔV, the Clausius-Clapeyron equation [48] may be used to calculate dP/dT. The dP/dT values in the transformations of alkali sulphates and nitrates are positive.

TABLE II Reversible phase transformations of alkali nitrates.

$M\mathrm{NO}_3$ M	Transformation	T_p^f (°C)	T_p^r (°C)	ΔH° (cal/mole)	E_a (kcal/mole)	ΔV (cm^3/mole)
Na	Rhombohedral (α) [33-35] → rhombohedral (α)	272	272	100	—	1.72
K	Orthorhombic (II) [36-38] → rhombohedral (I)	136	—	1200	110	0.83
	Rhombohedral (I) → rhombohedral (III)	—	118	820	—	—
	Rhombohedral (III) → orthorhombic (I)	—	96	380	—	—
Rb	Trigonal (IV) cubic (III) [39] hexagonal (II) cubic (I)					
	IV → II	166	153	950	165	2.52
	III → II	228	202	650	50	6.0
	II → I	278	270	300	55	3.12
Cs	Hexagonal (II) → cubic (I) [40]	161	149	350	75	3.19

TABLE III Reversible phase transformations of some inorganic substances.

Compound	Transformation	T_p^f (°C)	T_p^r (°C)	$\Delta H°$ (cal/mole)	ΔV (cm^3/mole)
Quartz	Hexagonal (β) → hexagonal (α')	575	5748	86 [9]	1.33
CsCl	Cubic (P*m*3*m*) → cubic (F*m*3*m*) [49]	479	446	580 [11]	10.28
Agl	Hexagonal (II) → cubic (I)	154	130	1470 [50]	−1.72 (−2.2)
NH_4Cl	Cubic (P*m*3*m*) → cubic (F*m*3*m*)	196	161	1073 [51]	7.14
NH_4Br	Cubic (P*m*3*m*) → cubic (F*m*3*m*)	179	155	882 [51]	9.50
$NaNO_2$	Orthorhombic (β) → orthorhombic (β')	166	160	250	1.66 [52]
$AgNO_3$	Orthorhombic (II) → hexagonal (I)	167	141	920	−0.50 [53]
$YbBO_3$	Hexagonal (α) → hexagonal (α') [54]	970	540	—	—

3.5. Thermal Hysteresis in Reversible Transformations

In the reversible transformations of alkali sulphates and nitrates (tables I and II), it can be seen that the transformation temperatures in the forward and reverse directions are different, the value in the latter case always being lower. The observation of different transformation temperatures in the directions is not consistent with the idea of true thermodynamic reversibility, and it is important to explain the temperature hysteresis, ΔT^h $(= T^f - T^r)$, in such reversible transformations. The observation of ΔT^h is a necessary consequence of the coexistence of the two phases [56]. The magnitude of ΔT^h varies from transformation to transformation, and in some cases it is found to be extremely large. A cursory examination indicated that the magnitude of ΔT^h was in some way related to the ΔV of the transformations. Thus, the α-β inversion of quartz [9], which is accompanied by very small ΔT^h, also shows a small ΔV.

In order to be able to carry out various possible correlations of ΔT^h, ΔV, and other parameters, a number of other reversible transformations were examined by DTA; the results are given in table III, where ΔV data for these transformations are also included. The temperature hysteresis, ΔT^h, may be viewed in terms of the hysteresis loop by plotting the fraction of the material transformed against temperature. A few typical hysteresis loops are shown in fig. 2.

If one were to propose that the two phases exist in thermal equilibrium over a temperature range, there must be two separate free energy-temperature curves for the forward and reverse transformations, and the average free energy of the transformation may be considered to be given by the tangent to the two free energy-temperature curves for the two phases [55].

The hysteresis loop itself may arise due to some "internal friction" [56a], where the heat flow to the crystal in the forward direction is different from the heat flow from the crystal in the reverse direction. In transformations where there are appreciable changes in volume, the heat flow to the crystal is associated with the expansion against a finite resistance. In the absence of any friction, there would be no hysteresis, and the transformation would be truly thermodynamically reversible. Many transformations are likely to proceed with slow nucleation associated with formation of isolated domains of a new phase, and the transformation may proceed later by a migration of the domain wall. Since the migration of a domain wall during a transformation involves mechanical work, it will not be possible to convert all of the heat into work [55], and there should necessarily be thermal hysteresis loss given by the area of the loop (table IV). It appears, therefore, that all crystal structure transformations involving volume changes should exhibit hysteresis.

In the literature, some attempts have been

TABLE IV Strain energy and other data on reversible phase transformations of various inorganic substances.

Transformation	ΔT_i^o	ΔT_p^o	ΔV (cm³/mole)	$\Delta T_i \Delta S$ (cal/mole)	E_s (cal/mole)	A^h
Li_2SO_4 II → I	4	35	3.81	32.55	325	33
K_2SO_4 ($\beta \rightarrow \alpha$)	<1	8	1.55	<2.0	1850	—
CsCl ($Pm3m \rightarrow Fm3m$)	13	33	10.28	10.40	830	45
Quartz ($\alpha - \beta$)	<0.5	0.7	1.33	<0.05	1176	10
$RbNO_3$						
IV → III	3	13	2.52	6.66	1195	16
III → II	8	26	6.0	12.8	—	37
II → I	1	8	3.12	0.55	860	6.5
$CsNO_3$ (II → I)	1	12	3.13	2.0	780	12.5
NH_4Cl ($Pm3m \rightarrow Fm3m$)	22	35	7.14	52.36	490	56
NH_4Br ($Pm3m \rightarrow Fm3m$)	19	24	9.50	41.61	590	56
AgI (II → I)	12	24	−2.2	42.72	450	27
$AgNO_3$ (II → I)	16	26	−0.5	33.92	200	17
$NaNO_2$ (II → I)	<1	6	1.66	<0.05	830	—

made to explain thermal hysteresis in transformations. Schäfer [57] considered thermal hysteresis as arising from the relatively small domain sizes, while Dinichert [58] and Frank and Wirtz [59] explained this on the basis of the different densities of the two phases, causing a strain energy. Staveley [60] has proposed a model based on Turnbull's theory of nucleation from melts, where the initial growth of the new phase is hindered by the interphase surface free energy and the strain to which the growing phase is subjected. There are some common features in the last three approaches, but none of these could clearly correlate the hysteresis to any measurable or understandable parameter. The only attempt of correlation was by Staveley [60], who pointed out that the thermal hysteresis (and the strain energies) may be related to the difference in the volumes of the two phases, ΔV. Since considerable data is available from the present study, it was considered interesting to examine if the observed hysteresis loop areas (fig. 2) are related to ΔV. The loop areas (table IV) represent the hysteresis loss, and by suitably multiplying the area by the difference in specific heats the loss may be obtained in energy units. A plot of A^h against ΔV (fig. 3) seems to indicate some proportionality. Although it was indicated that the thermal hysteresis in reversible phase transformations

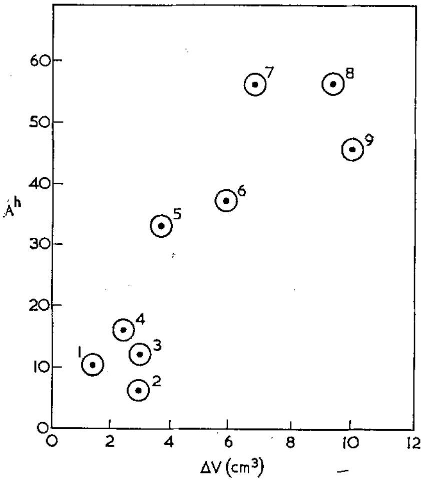

Figure 3 Plot of hysteresis loss (loop area) against change in molar volume in the transformation: (1) quartz ($\alpha \rightarrow \beta$); (2) $RbNO_3$(II → I); (3) $CsNO_3$(II → I); (4) $RbNO_3$(IV → III); (5) Li_2SO_4(II → I); (6) $RbNO_3$(III → II); (7) NH_4Cl ($Pm3m \rightarrow Fm3m$); (8) NH_4Br (bcc → fcc); (9) CsCl ($Pm3m \rightarrow Fm3m$).

may be related to ΔV, it was considered worthwhile to examine the origin of the hysteresis from kinetic, thermodynamic, and other considerations.

If one considers the potential energy diagram of an endothermic transformation, it can be seen that the transformation temperature for the reverse (exothermic) transformation should necessarily be lower than that in the forward direction, if the enthalpy change, the energy of activation, and the frequency factor, A, are taken to be nearly consistant

$$k^{\mathrm{f}} = A \exp(-E_{\mathrm{a}}^{\mathrm{f}}/\mathrm{R}T^{\mathrm{f}}) \qquad (1)$$

$$k^{\mathrm{r}} = A \exp(-E_{\mathrm{a}}^{\mathrm{r}}/\mathrm{R}T^{\mathrm{r}}) \qquad (2)$$

Since $E_{\mathrm{a}}^{\mathrm{f}} - E_{\mathrm{a}}^{\mathrm{r}} = \Delta H^0$, for reversible transformations, T^{r} should be less than T^{f} at isokinetic points. In many reversible transformations of the first order, the E_{a} values are much too large compared to ΔH^0, and it will not be possible to account for the large thermal hysteresis ΔT^{h}, observed in these transformations, on the basis of the above considerations alone.

If an additional term involving strain energy [56] is included in the rate expression, then the strain energies associated with the forward and reverse transformation would be considerably different, since the ΔV will be quite different in the two directions. In the case of the forward transformation with positive ΔV, nuclei of lower density have to grow in a matrix of higher density giving rise to fairly large strain energies, while in the reverse direction it is just the opposite and the strain energy should be comparatively small.

$$k^{\mathrm{f}} = A \exp -(E_{\mathrm{a}}^{\mathrm{f}} + E_{\mathrm{s}}^{\mathrm{f}})/\mathrm{R}T^{\mathrm{f}} \qquad (3)$$

$$k^{\mathrm{r}} = A \exp -(E_{\mathrm{a}}^{\mathrm{r}} + E_{\mathrm{s}}^{\mathrm{r}})/\mathrm{R}T^{\mathrm{r}} \qquad (4)$$

Where E_{s} is the strain energy and $E_{\mathrm{s}}^{\mathrm{f}} \gg E_{\mathrm{s}}^{\mathrm{r}}$. Under these conditions, one would get a fairly large thermal hysteresis, ΔT^{h}. Assuming $E_{\mathrm{a}}^{\mathrm{f}}$ as nearly equal to $E_{\mathrm{a}}^{\mathrm{r}}$ and $T^{\mathrm{f}} \approx T^{\mathrm{r}} \approx T^{\mathrm{m}}$ (median temperature)

$$k^{\mathrm{f}}/k^{\mathrm{r}} \approx \exp(-\Delta E_{\mathrm{s}}/\mathrm{R}T^{\mathrm{m}}) \qquad (5)$$

Further, $k^{\mathrm{f}} \propto 1/t^{\mathrm{f}}_{\infty}$ and $k^{\mathrm{r}} \propto 1/t^{\mathrm{r}}_{\infty}$, where t^{f}_{∞} and t^{r}_{∞} stand for the times required for the completion of the transformation in the forward and reverse directions. If one employs a constant rate of heating or cooling in a DTA experiment, the terms t^{f}_{∞} and t^{r}_{∞} may be replaced by $\Delta T_{\mathrm{pi}}^{\mathrm{f}}$ $(= T_{\mathrm{p}}^{\mathrm{f}} - T_{\mathrm{i}}^{\mathrm{f}})$ and $\Delta T_{\mathrm{ip}}^{\mathrm{r}}$ $(= T_{\mathrm{i}}^{\mathrm{r}} - T_{\mathrm{p}}^{\mathrm{r}})$. Thus,

$$K^{\mathrm{f}}/k^{\mathrm{r}} = \exp(-\Delta E_{\mathrm{s}}/\mathrm{R}T^{\mathrm{m}}) = \Delta T_{\mathrm{ip}}^{\mathrm{r}}/\Delta T_{\mathrm{pi}}^{\mathrm{f}} \qquad (6)$$

The strain energy term, ΔE_{s}, can thus be evaluated with the knowledge of T_{i} and T_{p} in the forward and reverse directions. Calculations of ΔE_{s} by this procedure would, however, be difficult in the case of transformations which take place over a wide range of temperatures (only data of T_{p} can be obtained from the DTA curves of such transformations). The values of ΔE_{s} calculated for various transformations by the above procedure are given in table IV.

It is important that the actual value of thermal hysteresis, ΔT^{h}, be properly defined. If one takes ΔT^{h} as equal to the difference in the transformation temperatures in the forward and reverse directions after completion of a transformation $(\Delta T_{\mathrm{p}}^{\mathrm{h}} = T_{\mathrm{p}}^{\mathrm{f}} - T_{\mathrm{p}}^{\mathrm{r}})$, then the ΔT^{h} would include kinetic factors. A proper definition should probably be $\Delta T_{\mathrm{i}}^{\mathrm{h}} = T_{\mathrm{i}}^{\mathrm{f}} - T_{\mathrm{i}}^{\mathrm{r}}$, since this would exclude contributions arising from the differences in the kinetics of transformations (and therefore the strain energies) in the two directions. In table IV, both the values of ΔT^{h} have been shown.

Since the values of the strain energy, ΔE_{s}, have been obtained by a treatment of the data from the DTA curves, it is likely that these values are approximate, but they would still be useful for purposes of comparison among a number of reversible transformations. To ascertain that changes in rates of heating do not alter ΔE_{s} values, the ΔE_{s} values for the P*m*3*m* → F*m*3*m* transformations of ammonium chloride were examined with different rates of heating.

Rate of heating (°C/min)	*Rate of cooling* (°C/min)	ΔE_{s} (cal/mole)
4	6	440
8	6	450
16	6	380

It can be seen that ΔE_{s} values are roughly in the same region, and the variation is ±100 cal. The ΔE_{s} data in table IV were, however, obtained by employing conditions where rates of heating and cooling were nearly the same.

Recent studies on zirconia [61] have shown that a metastable phase occurs as a crystallite size effect. In order to examine the possible dependence of ΔE_{s} and other parameters from DTA curves on the particle size (surface free energy), the ΔE_{s} values were calculated for the transformations of caesium chloride and ammonium chloride with different particle sizes and the results are given below.

Compound	*Particle size* (μm)*	ΔE_s (cal/mole)	ΔH^0 (cal/mole)
CsCl	417 to 295	879	580
	295 to 147	770	580
	<147	920	620
NH_4Cl	295 to 147	370	1070
	<147	460	1130

*employing ASTM standard sieves

It can be seen that the values of ΔE_s and ΔH^0 are not very sensitive to particle size and the variations in ΔE_s are within ±100 cal/mole.

The plot of ΔE_s of various transformations (table IV) against ΔV is shown in fig. 4. The shape of the curve indicates that the strain energy is minimum at a particular value of ΔV. A similar curve is obtained if ΔE_s is plotted against $\Delta V^{\frac{1}{3}}(=\Delta r)$, where Δr may be taken to represent differences in the sizes of the spherical nuclei of the parent and transformed phases. It is difficult to interpret the shape of the curve in fig. 4. In the correlations of ΔE_s, or the area of the hysteresis loop, A^h, with ΔV, no justification was given hitherto for employing ΔV as the parameter. It is possible to derive an expression for the strain energy from theories of elasticity where singularities in the strain distribution are discussed in terms of the action of singular forces [62]. In the case where three double forces without moment are operating at a centre of compression or dilatation, the strain, ϵ_{rr}, and stress, σ_{rr}, are given by [62]:

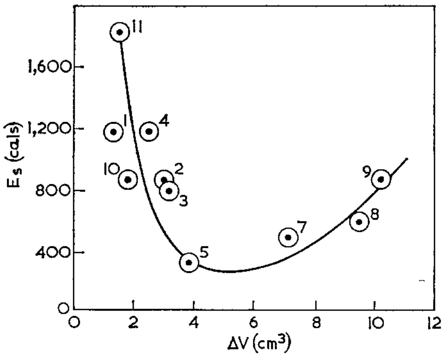

Figure 4 Plot of the strain energy against the change in molar volume in the transformation. The numbers shown in the figure correspond to the same transformations as in fig. 3; plus (10) $NaNO_2$ (II → I) and (11) K_2SO_4 ($\beta \rightarrow \alpha$).

$$\sigma_{rr} = \frac{8\pi}{3} G \left(\frac{1+\nu}{1-2\nu}\right) E r_0^3 \left(\frac{1-2\nu}{1-\nu}\right) \frac{1}{r^3} \quad (7)$$

$$\epsilon_{rr} = \frac{8\pi}{3} G \left(\frac{1+\nu}{1-2\nu}\right) E r_0^3 \frac{1}{8\pi G} \left(\frac{1-2\nu}{1-\nu}\right) \frac{1}{r^3} \quad (8)$$

where G is the modulus of rigidity, ν Poissons ratio, and r the radius of a nucleus. The radius r is $(1 + E)$ times as large as r_0. If ϵ_{rr} is written as equal to $k\ E(r_0^3/r^3)$, and σ_{rr} as equal to $k'G\ E(r_0^3/r^3)$, where k and k' are constants, then the strain energy, E_s, will be:

$$E_s = \int_{r_0}^{R} \sigma_{rr}\, \epsilon_{rr}\, 4\pi r^2\, \mathrm{d}r \quad (9)$$

$$= k''\, G \int_{r_0}^{R} E^2 \frac{r_0^6}{r^4}\, \mathrm{d}r \quad (10)$$

where R is the maximum radius of the nucleus under strain. Since $R \gg r_0$,

$$\begin{aligned} E_s &= k'''\, G\, r_0\, \Delta r^2 \\ &= k'''\, G\, V_i^2\, \Delta V^{2/3} \end{aligned} \quad (11)$$

Where V_i is the volume of the parent (transforming) unit cell.

The above derivation shows that the strain energy is in some way related to a ΔV term. Unfortunately, equation 11 could not be employed for correlations of ΔE_s or A^h in the present study, since elastic constant (G) data on these inorganic substances are not available in the literature.

Till now, the strain energy has been derived from kinetic data and shown to be related to volume factors in transformations. It was considered worthwhile to examine how this strain energy is related to themodynamic state and energy functions. If one considers the thermodynamics of reversible crystal transformations, a few interesting features become apparent. At equilibrium,

$$(\Delta H - T\Delta S)^f + E_s^f = (\Delta H - T\Delta S)^r + E_s^r \quad (12)$$

Since $\Delta H_{tr}^f = -\Delta H_{tr}^r$

$$E_s = E_s^f - E_s^r = -2\,\Delta H + T^f\,\Delta S^f - T^r\,\Delta S^r \quad (13)$$

Assuming $\Delta S \approx -\Delta S^f \approx \Delta S^r$

$$\Delta E_s = -2\,\Delta H + \Delta S\,(T^f + T^r)$$

or $$E_s = -2\,\Delta H + \Delta S\,(2T^f - \Delta T) \quad (14)$$

Thus $$\Delta E_s = -\Delta S\,\Delta T \quad (15)$$

It was found that plots of hysteresis loss, A^h, as well as the strain energy, ΔE_s, against ΔS ΔT_i of transformation were similar to those found, when these were plotted against ΔV (figs. 3 and 4).

4. Concluding Remarks

Differential thermal analysis can be used satisfactorily for quantitative evaluation of the enthalpy changes in crystal structure transformations, if the transformations are accompanied by large energy changes (as in first order or reconstructive transformations). The enthalpy data obtained for transformations taking place over a wide range of temperatures could be erroneous. Data on the kinetics of the transformation obtained from DTA curves, though not quantitative (probably have large uncertainties), serve as useful measures for comparing data on a related series of transformations. DTA is a useful tool for the study of thermal or structural hysteresis in reversible transformations. The thermal hysteresis can be studied easily and quantitatively by this technique.

Although the studies reported here have not been able to solve the problem of thermal hysteresis in reversible transformations completely, two important conclusions seem to be possible.

(a) Thermal hysteresis, ΔT^h, is related to the differences in volumes of the parent and the transformed phases, ΔV. The hysteresis loss is nearly linear with respect to ΔV. Thermal hysteresis should necessarily accompany reversible transformations where volume changes take place against a finite resistance.

(b) One can relate the thermal hysteresis in transformations to the strain energy, ΔE_s. The strain energy can approximately be evaluated from DTA curves recorded under controlled conditions. Strain energy appears to be a function of ΔV, as can be shown from arguments based on theories of elasticity. ΔE_s is also related to $\Delta T \Delta S$, as can be shown from thermodynamic considerations. These results may be of value in the study of transformations of importance in metallurgy.

Acknowledgements

The authors are thankful to the National Bureau of Standards, USA (Special International Projects), for the grant of a research project (NBS (G)-51). The authors are also thankful to Dr M. N. Setty of the Department of Metallurgical Engineering, Indian Institute of Technology, Kanpur, for valuable discussions on problems relating to elasticity.

References

1. A. F. WELLS, "Structural Inorganic Chemistry" (Clarendon Press, Oxford, 1962).
2. L. PAULING, "Nature of the Chemical Bond" (Cornell University Press, Ithaca, New York, 1960).
3. H. J. BORCHARDT, *J. Chem. Ed.* **33** (1956) 103.
4. S. GORDON, *J. Chem. Ed.* **40** (1963) A87.
5. J. A. PASK, University of California, Institute of Research Publications, Series 18, Issue 3 (1952).
6. R. L. N. SASTRY, S. R. YOGANARASIMHAN, P. N. MEHROTRA, and C. N. R. RAO, *J. Inorg. Nucl. Chem.* **28** (1966) 1165.
7. A. ARELL, *Ann. Acad. Sci. Fenn.* AVI, No. 101 (1962).
8. A. ARELL and M. VARTEVA, *Ann. Acad. Sci. Fenn.* AVI, No. 88 (1961).
9. A. J. MAJUMDAR, H. A. MCKINSTRY, and R. ROY, *J. Phys. Chem. Solids* **25** (1964) 1487.
10. A. J. MAJUMDAR and R. ROY, *J. Phys. Chem.* **69** (1965) 1684.
11. K. J. RAO, G. V. S. RAO, and C. N. R. RAO, *J. Phys. Chem. Solids* (in press).
12. H. J. BORCHARDT and F. DANIELS, *J. Am. Chem. Soc.* **79** (1957) 41.
13. T. FORLAND and J. KROGH-MOE, *Acta Chem. Scand.* **11** (1957) 565.
14. L. K. FREVEL, *J. Chem. Phys.* **8** (1940) 290.
15. H. FISCHMEISTER, *Acta Cryst.* **7** (1954) 776.
16. W. H. ZACHARIASEN and G. E. ZEIGLER, *Z. Krist.* **81** (1932) 92.
17. M. A. BREDIG, *J. Am. Chem. Soc.* **63** (1941) 2533.
18. R. MOREAU, *Bull. Soc. Roy. Sci.* (Liege) **32** (1963) 252.
19. M. BERNARD and R. HOCART, *Bull. Soc. Franc. mineral. Crist.* **84** (1961) 396.
20. F. P. GOERDER, *Proc. Natl. Acad. Sci.* **13** (1927) 793.
21. A. OGG, *Phil. Mag.* **5** (1) (1928) 354.
22. H. F. FISCHMEISTER, *Monatsh. Chem.* **93** (1962) 420.

23a. J. P. COUGHLIN, *J. Am. Chem. Soc.* **77** (1955) 868.

23b. H. F. FISCHMEISTER, *Z. Physik. Chem.* **7** (1956) 94.

24. F. C. KRACEK, *J. Phys. Chem.* **33** (1929) 1281.
25. F. C. KRACEK and R. E. GIBSON, *J. Phys. Chem.* **34** (1930) 188.
26. C. MAZIERES, *Ann. Chim.* (1961) 576.
27. F. C. KRACEK and C. J. KSANDA, *J. Phys. Chem.* **34** (1930) 1741.
28. M. A. BREDIG, *J. Phys. Chem.* **47** (1943) 587.
29. M. A. BREDIG, *J. Phys. Chem.* **49** (1945) 543.
30. V. M. GOLDSCHMIDT, "Geochemische Verteilungsgesetze," Volume VII (Oslo, 1926), p. 105.
31. R. E. WESTON, Jr and T. F. BRODASKY, *J. Chem. Phys.* **27** (1957) 683.

32a. L. PAULING, *Phys. Rev.* **30** (1930) 430.
32b. M. J. BUERGER, *Fortschr. Miner.* **39** (1961) 9.
33a. F. C. KRACEK and E. POSNJAK, *J. Am. Chem. Soc.* **53** (1931) 1183.
33b. F. C. KRACEK, *ibid*, 2609.
33c. F. C. KRACEK, E. POSNJAK, and S. B. HENDRICKS, *ibid*, 3339.
34. P. E. TAHVONEN, *Ann. Acad. Sci. Fenn.* Series AI, No. 43 (1946).
35. M. KANTOLA and E. VILHONEN, *Ann. Acad. Sci. Fenn.* Series AVI, No. 54 (1960).
36a. F. C. KRACEK, *J. Phys. Chem.* **34** (1930) 225.
36b. F. C. KRACEK, T. F. W. BARTH, and C. J. KSANDA, *Phys. Rev.* **40** (1932) 1034.
37. C. FINBAK and O. HASSEL, *Z. Phys. Chem.* **B37** (1937) 75.
38. F. W. BARTH, *Z. Phys. Chem.* **B43** (1939) 448.
39. R. N. BROWN and A. C. MCLAREN, *Acta Cryst.* **15** (1962) 974.
40. C. FINBAK and O. HASSEL, *J. Chem. Phys.* **5** (1937) 460.
41. S. SHOZO, N. SHOICHIRO, and F. SHIMICHI, *J. Phys. Soc. Japan* **13** (1958) 1549.
42. A. L. KHODAKOV and E. Z. MIRSKAYA, *Krystallographia* **7** (1962) 477.
43. I. S. ZHELUDEV and A. S. SONIN, *Izvest. Acad. Nauk. SSSR* Ser. Fiz. **22** (1958) 1441.
44. A. Y. DANTSIGER, Nauchn. Konf. Aspirantov, (1962) 75.
45. H. FROHLICH, *Archiv. Sci.* **10** Spec. No. 5-6 (1957).
46. R. K. KHANNA, J. LINGSCHEID, and J. C. DECIUS, *Spectrochim. Acta* **20** (1964) 1109.
47. G. B. RAVICH and B. N. ERGOV, *Zhur. Neorg Khim* **5** (1960) 2603.
48. S. GLASSTONE, "Thermodynamics for Chemists" (Van Nostrand, New York, 1958).
49. J. W. MENARY, A. R. UBBELOHDE, and I. WOODWARD, *Proc. Roy. Soc.* (London) **A208** (1961) 158.
50. A. J. MAJUMDAR and R. ROY, *J. Phys. Chem.* **63** (1959) 1858.
51. A. ARELL, *Ann. Acad. Sci. Fenn.* Series AVI, No. 57 (1960).
52. S. TANISAKI, *J. Phys. Soc. Japan* **18** (1963) 1181.
53. R. W. G. WYCKOFF, "Crystal Structures" (Interscience, New York, 1960).
54. E. M. LEVIN, R. S. ROTH and J. B. MARTIN, *Am. Mineral.* **46** (1961) 1035.
55. C. J. SCHNEER and R. W. WHITING, *Am. Mineral.* **48** (1963) 737.
56. A. R. UBBELOHDE, *Quart. Rev.* **11** (1957) 246.
56a. A. H. COTTRELL, "Dislocations and Plastic Flow in Crystals" (Clarendon press, Oxford, 1963).
57. K. SCHÄFER, *Z. Physical Chem.* **42B** (1939) 127.
58. P. DINICHERT, *Helv. Physica Acta* **17** (1944) 389.
59. F. C. FRANK and K. WIRTZ, *Naturwiss.* **42** (1938) 687.
60. D. C. THOMAS and L. A. K. STAVELEY, *J. Chem. Soc.* **1420** (1951) 2572.
61. R. C. GARVIE, *J. Phys. Chem.* **69** (1965) 1238.
62. H. G. VAN BUEREN, "Imperfections in Crystals" (North Holland, Amsterdam, 1960), Ch. IV, p. 94.